



# Code of Practice: Small Punch Testing of reference material BCR-661 (Nimonic 75)

*Open Access to JRC Research Infrastructures; 2020-1-RD-EMMA-SMPA, SPT-INVEST*

Holmström, S., Brynk, T., Simonovski, I., Baraldi, D.

2024

OPEN ACCESS  
to JRC Research Infrastructures

EUR 31931

Joint  
Research  
Centre

This document is a publication by the Joint Research Centre (JRC), the European Commission's science and knowledge service. It aims to provide evidence-based scientific support to the European policymaking process. The contents of this publication do not necessarily reflect the position or opinion of the European Commission. Neither the European Commission nor any person acting on behalf of the Commission is responsible for the use that might be made of this publication. For information on the methodology and quality underlying the data used in this publication for which the source is neither Eurostat nor other Commission services, users should contact the referenced source. The designations employed and the presentation of material on the maps do not imply the expression of any opinion whatsoever on the part of the European Union concerning the legal status of any country, territory, city or area or of its authorities, or concerning the delimitation of its frontiers or boundaries.

#### Contact information

Name: Igor Simonovski

Email: igor.simonovski@ec.europa.eu

#### EU Science Hub

<https://joint-research-centre.ec.europa.eu>

JRC137398

EUR 31931 EN

PDF ISBN 978-92-68-15570-7 ISSN 1831-9424 doi:10.2760/77274

KJ-NA-31-931-EN-N

Luxembourg: Publications Office of the European Union, 2024

© European Atomic Energy Community, 2024



The reuse policy of the European Commission documents is implemented by the Commission Decision 2011/833/EU of 12 December 2011 on the reuse of Commission documents (OJ L 330, 14.12.2011, p. 39). Unless otherwise noted, the reuse of this document is authorised under the Creative Commons Attribution 4.0 International (CC BY 4.0) licence (<https://creativecommons.org/licenses/by/4.0/>). This means that reuse is allowed provided appropriate credit is given and any changes are indicated.

For any use or reproduction of photos or other material that is not owned by the European Atomic Energy Community permission must be sought directly from the copyright holders.

How to cite this report: European Commission, Joint Research Centre, Holmström, S., Brynk, T., Simonovski, I. and Baraldi, D., *Code of Practice: Small Punch Testing of reference material BCR-661 (Nimonic 75)*, Publications Office of the European Union, Luxembourg, 2024, <https://data.europa.eu/doi/10.2760/77274>, JRC137398.

**Contents**

Foreword.....1

Acknowledgements .....2

Abstract.....3

Research visits and assessment work.....4

1 Introduction.....5

2 Material .....6

3 SP test results .....9

4 FEA simulations .....12

    4.1 Constitutive law .....12

    4.2 FEA model.....15

5 Test data assessment for proof and tensile strength.....20

6 Test results and SP correlation parameters based on the reference material verified tensile properties.....22

7 Conclusion.....27

Glossary, abbreviations and definitions as given in [4].....28

List of figures .....30

List of tables.....31

References.....32

## **Foreword**

This report presents the assessment of the reference material BCR-661 (Nimonic 75) tested within the SPT-INVEST open access project. It is intended as a Code of Practice (COP) for using the Nimonic 75 material, currently used as reference material for conventional uniaxial tensile and creep test verification, as a reference also for Small-Punch (SP) testing. The report can be used for laboratory specific test set-up verification, assessment calibration, as well as comparing results on the basis of expected effects of friction between ball and test piece. The COP is also intended for inter-laboratory round robin use for further qualification of the reference material for SP, and eventually to be proposed for incorporation in the EN standard EN-10371.

## **Acknowledgements**

Authors would like to acknowledge Structural Materials Performance Assessment Laboratories (SMPA) staff support during testing, analysis and post-test evaluation of the results.

### In Memoriam

Tomasz Brynk (main tester and initiator of the SPT-INVEST project) has sadly passed away on the 28.7.2022. He will be sorely missed by us all.

### Authors:

Stefan Holmström (corresponding author, assessor)

Tomasz Brynk (initiator and test performer)

Igor Simonovski (test performer, data management and FEA support)

Daniele Baraldi (constitutive models)

## Abstract

One of the main aims of SPT-INVEST project was to assess the reference material BCR-661 (Nimonic 75) in greater detail with the aim of clarifying, if this reference material (which is according to the ISO 6892, Part 1 standard only for uniaxial tensile testing) would also be suitable for the small punch test (EN-10371). The test results and assessment reported here clearly indicate that for room temperature testing the material shows great potential. However, this report also shows that special attention has to be given to laboratory specific test set-up differences, e.g. puncher, receiving hole and chamfer actual dimensions. For proof strength estimation the chosen methodology for extracting the representative  $F_e$  forces has clearly different correlation coefficients and different sensitivity to the test piece thickness. For the tensile strength, estimations by correlation to the classical maximum force ( $F_m$ ) over the location of the maximum displacement  $v_m$  or deflection  $u_m$ , also result in uncertainties regarding the optimal correlation constant for the here tested specimen thickness range. This report gives the estimated friction coefficient for the JRC test lab specific test set-up, but suggests that future work still has to be performed in fine-tuning the models used by the finite element software, i.e. a damage model capable of catching the final plastic collapse stage of the SP tests. The here reported correlation coefficients for force to stress conversion still need further fine-tuning based on a larger data base. This is planned to be accomplished through an inter laboratory round-robin. The discussion part of this report includes some recommendations for the future round-robin exercise.

## **Research visits and assessment work**

Testing:

Tomasz Brynk (SCK CEN): 14.03.2022-18.03.2022

Stefan Holmström (SCK CEN): 14.03.2022-16.03.2022

Assessment and data management:

Stefan Holmström (SCK CEN): October 2022-January 2024

Igor Simonovski (JRC Petten): June 2022- February 2023

FEA simulations:

Igor Simonovski (JRC Petten): March 2022 and May 2024

# 1 Introduction

Small Punch Tests (SPT) is a promising method of mechanical properties determination for the cases where material amount is limited. However, due to a complex loading state during SPT, the results are not easily transferable to the uniaxial engineering material properties traditionally acquired by tensile testing. The methodology proposed in the small punch (SP) standard is utilizing empirical correlation factors that has been shown, for some materials, and perhaps some specific test set-up, to give sub-optimal tensile property estimates. Especially the estimation of proof strength shows a large scatter and sometimes large discrepancies. Several methodologies to improve the estimation accuracy are currently under development by various authors, e.g. [1], [2] and [3]. However, in this report only the classical methodologies are investigated.

The main aim of the assessment of the reference material BCR-661 (Nimonic 75) is to make a guideline, or Code of Practice (COP), to support the development of the SP test method by making available an initial set of Small Punch (SP) test curves with a detailed analysis. This work will hopefully lead to the generation of a well-established material properties data base. By analysing the data and quantifying the inherent data scatter and the effect on estimated properties, the first recommendations towards an inter-laboratory round-robin have been taken.

As described later in this report, the incorporation of also non-standard thicknesses is the basis for acquiring data that enables the estimation of the friction coefficient, when applied in comparison to Finite Element Analysis (FEA) simulations. The test data on test pieces of various thickness is here also used for showing the potential magnitude of estimation errors to be taken into account when applying constant or corrected correlation coefficients, e.g. those given in the informational annex of EN-10371 [4].

The report is the second report for the SPT-INVEST project, executed in close cooperation between SCK CEN and JRC Petten.

## 2 Material

The BCR-661 reference material tested by SP is a highly qualified material made available through Joint Research Centre (JRC) in Geel, Belgium. The BCR-661 is a specific material batch of Nimonic 75 [5][6] with a chemical composition given in Table 1. The material properties are given in Table 2. For the qualification of the tensile material properties for SP use, the verified true tensile material properties are chosen in this work [7].

**Table 1. Chemical analysis of 14 mm diameter reference material bars (mass %) as given in [5].**

	Bars					
	1	9	28	52	115	160
C	0.11	0.11	0.10	0.10	0.10	0.10
Si	0.38	0.37	0.37	0.40	0.41	0.43
Mn	0.41	0.41	0.41	0.41	0.41	0.41
Al	0.24	0.24	0.22	0.19	0.17	0.17
Co	0.16	0.16	0.16	0.16	0.16	0.16
Cr	18.8	18.8	18.8	18.8	18.8	18.8
Cu	0.20	0.20	0.21	0.21	0.21	0.21
Fe	3.99	3.99	4.00	4.00	4.00	4.01
Mo	0.08	0.08	0.08	0.08	0.08	0.08
Nb	0.03	0.03	0.03	0.03	0.03	0.03
Ti	0.30	0.30	0.30	0.28	0.27	0.26
V	0.02	0.02	0.02	0.01	0.01	0.01
Ni	rest	rest	rest	rest	rest	rest

**Table 2. Material properties according to the certificate of analysis [7].**

### BCR<sup>®</sup> - 661

NICKEL BASE ALLOY			
	Ambient temperature tensile properties		
	Certified value <sup>2)</sup>	Uncertainty <sup>3)</sup>	Unit
0.2 % Proof stress ( $R_{p0.2}$ ) <sup>1)</sup>	300	8	MPa
0.5 % Proof stress ( $R_{p0.5}$ ) <sup>1)</sup>	318	7	MPa
Tensile strength ( $R_m$ ) <sup>1)</sup>	750	14	MPa
Elongation at fracture (A) <sup>1)</sup>	40.9	0.9	%
Reduction in area at fracture (Z) <sup>1)</sup>	60	4	%

1) As defined in EN 10002-1.  
2) Certified values are values that fulfil the highest standards of accuracy. The given value(s) represent(s) the unweighted mean value of the means of accepted sets of data, each set being obtained in a different laboratory and/or with a different method of determination. The certified value and its uncertainty are traceable to the International System of units (SI).  
3) The uncertainty is the expanded uncertainty of the certified value with a coverage factor  $k = 2$  corresponding to a level of confidence of about 95 % estimated in accordance with ISO/IEC Guide 98-3, Guide to the Expression of Uncertainty in Measurement (GUM:1995), ISO, 2008.

The SP test pieces of the Nimonic 75 (BCR-661) that are used in this work are coded as the EU series, as defined by the JRC-Petten test piece coding structure. The test pieces were fabricated by SCK CEN through extraction from the reference material, 14 mm diameter rods purchased from the JRC reference laboratory in Geel, Belgium in the L – direction (see Figure 1). The SP test pieces were fabricated by first machining the rods to a diameter of 8 mm and then EDM (Electrical Discharge Machining) cut from the cylinders to a thickness of approximately 0.6 mm in thickness. The EDM cut disks were then polished manually from both sides to remove any EDM damaged material to reach their final target thicknesses, finalizing the polishing by 1200 grit abrasive

paper to reach the standardized surface roughness. The final thicknesses, Table 3, are targeted to be within the pre-defined thickness levels of 0.450, 0.500 and 0.550 mm with a maximum standard deviation of 1%. The test pieces were measured for thicknesses at five (5) locations each. Since the objectives and target of the SPT-INVEST project required sufficiently different test piece thicknesses, the acquired test piece quality was considered sufficient for purpose, even for the thinnest test piece (EU-17) with one outlying thickness result (out of 5) as shown in Figure 2.

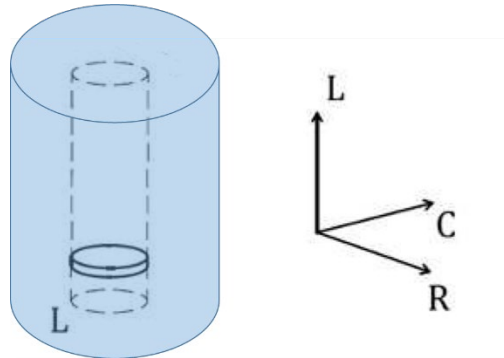


**Figure 1. Test piece extraction from Nimonic 75 (BCR-661) rod.**

**Table 3. Test piece identification codes, ordered by measured thicknesses, the original measurement performed at SCK CEN with a 10  $\mu\text{m}$  resolution and re-measured at JRC with a 1  $\mu\text{m}$  resolution.**

ID code	Thickness (mm) Orig. SCK CEN meas.	Thickness (mm) JRC meas. 5 positions	Note
EU-17	0.430	0.431 $\pm$ 2.1%	Full test [8]
EU-15	0.445	0.448 $\pm$ 0.5%	Full test [9] <sup>1</sup>
EU-06	0.490	0.485 $\pm$ 0.8%	Full test [10]
EU-04	0.495	0.498 $\pm$ 0.3%	Full test [11] <sup>2</sup>
EU-07	0.520	0.523 $\pm$ 0.7%	Full test [12]
EU-09	0.560	0.556 $\pm$ 1.0%	Full test [13]
EU-13	0.450	0.452 $\pm$ 0.5%	Interrupted test at $u=1.1$ mm [14]
EU-01	0.495	0.501 $\pm$ 0.7%	Interrupted test at $u=1.1$ mm [15]
EU-08	0.555	0.557 $\pm$ 1.0%	Interrupted test at $u=1.1$ mm [16]

<sup>1</sup>Deflection sensor unresponsive until approximately 30 N at test beginning.

<sup>2</sup>Displacement has a 'tail' at the beginning of the test making trilinear extraction of  $F_e$  values necessary, the deflection only starts registering at approximately 30 N.

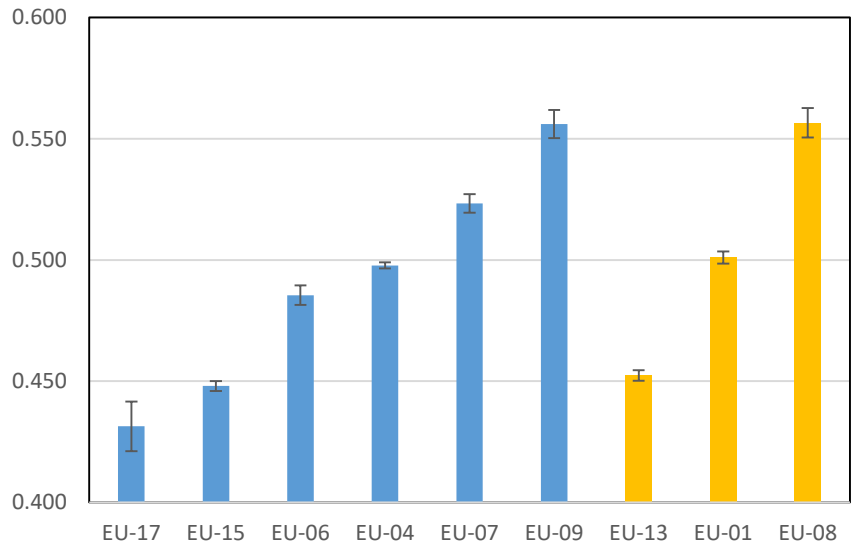


**Figure 2. Nimonic 75 (BCR-661) test piece thicknesses, blue test pieces used for full tests, yellow for interrupted tests.**

### 3 SP test results

The SP Force-Deflection curves for the reference material, tested at room temperature, are shown in Figure 3. The test pieces were tested at the SMPA JRC laboratory in Petten according to EN-10371 standard [4] at a cross head displacement rate of 0.5 mm / minute.

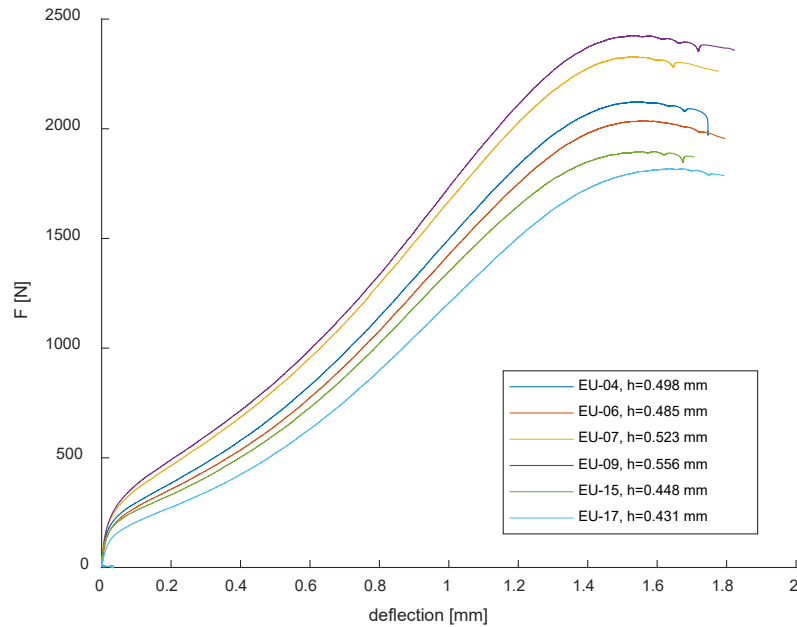


**Figure 3. Force-Deflection (F-u) curves at room temperature for the different test piece thicknesses.**

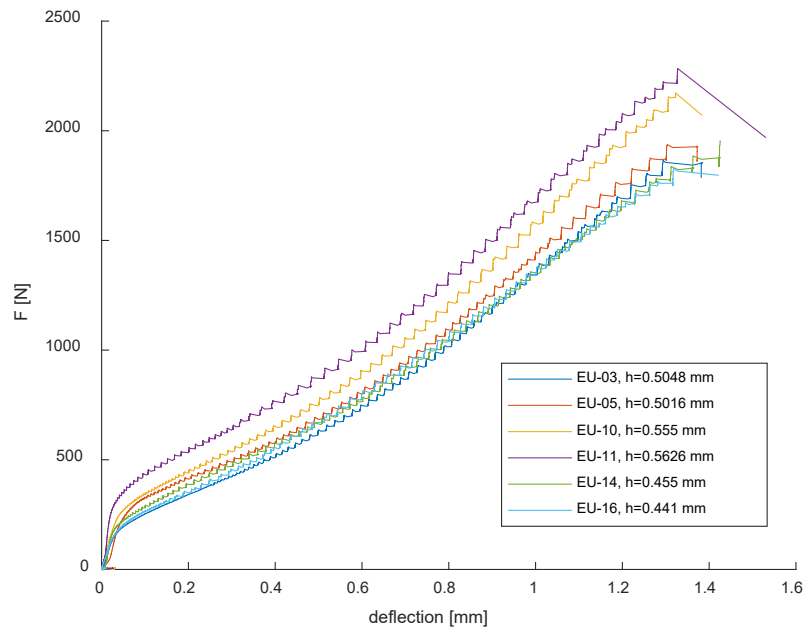


**Figure 4. Force-Deflection (F-u) curves at 450°C for the different test piece thicknesses [17], [18], [19], [20], [21], and [22].**

The three interrupted tests conducted at room temperature were performed for studying the ‘as tested’ deformation (with 3D profilometry) in comparison to FEA simulations. Initial results on the profilometry campaign are given in Figure 5 together with images of an interrupted test and a test conducted beyond the

maximum force. It is foreseen that the follow up collaboration between SCK CEN and JRC Petten will produce a more detailed journal paper on the profilometry results and FEA simulations in the near future.

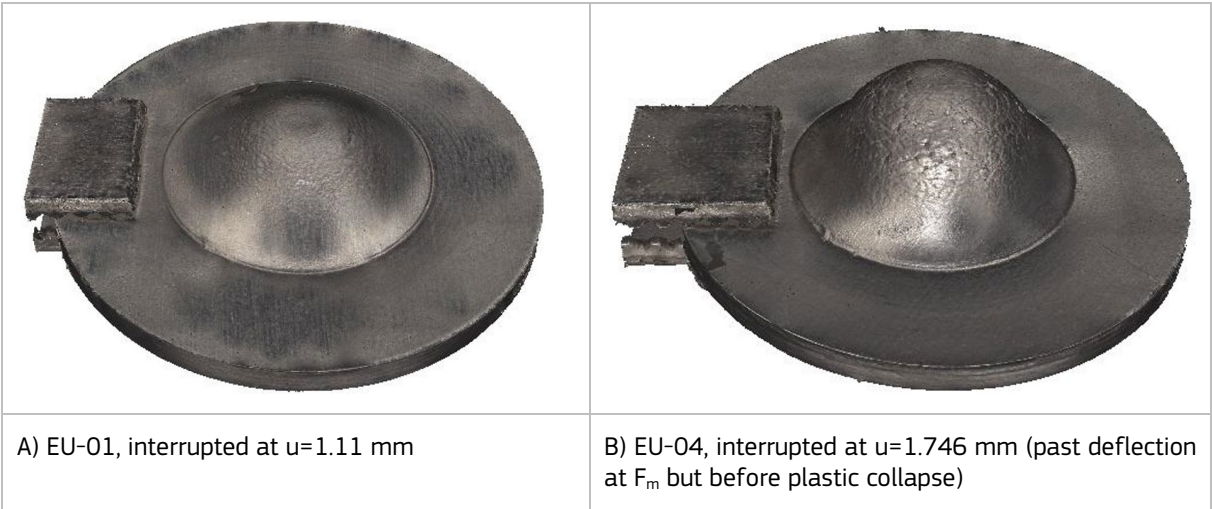


**Figure 5. Full 3D surface scan for Nimonic 75 (BCR-661) test piece. The 3D profilometer measured deflection  $u_{meas} = 1.080$  mm for the interrupted test and 1.624 mm for the full test. The corresponding LVDT measure values are 1.11 and 1.74 mm correspondingly.**

The Force-Deflection curves of the full and interrupted tests for the standard thickness of 0.5 mm are shown in Figure 6, and in Figure 7 and Figure 8 for the nominal thicknesses of 0.56 mm and 0.45 mm correspondingly. The full and interrupted test curves fall nearly perfectly on top of each other for the three test piece thicknesses, indicating that the material response is repeatable, as it should be for a reference material.

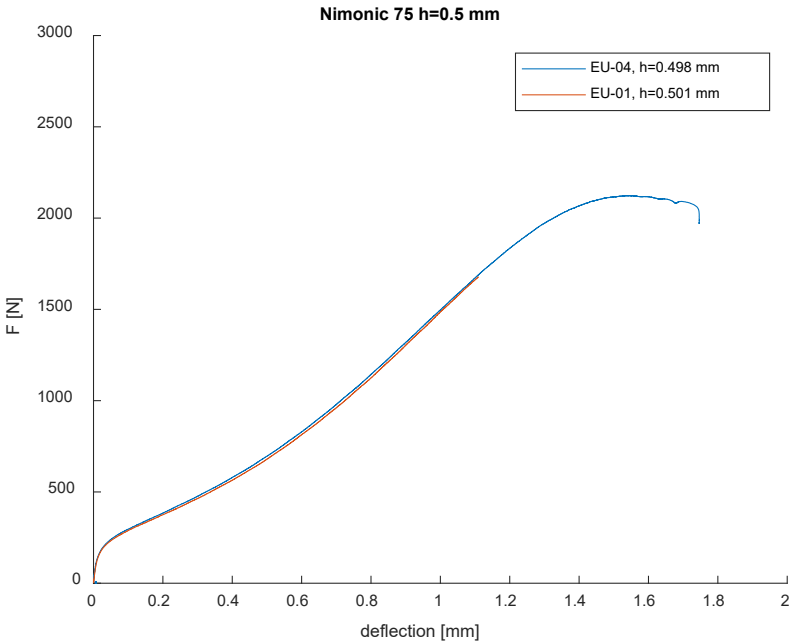


**Figure 6. Force-Deflection (F-u) curves for full and interrupted test with test piece thickness within  $0.5 \pm 0.05$  mm.**

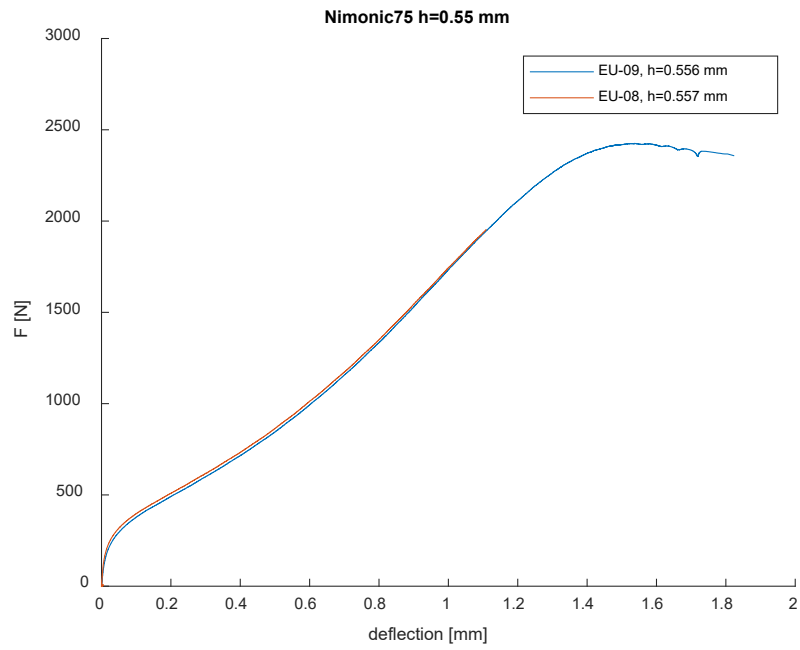


**Figure 7. Force-Deflection (F-u) curves for full and interrupted test with test piece thickness within  $0.56 \pm 0.05$  mm.**

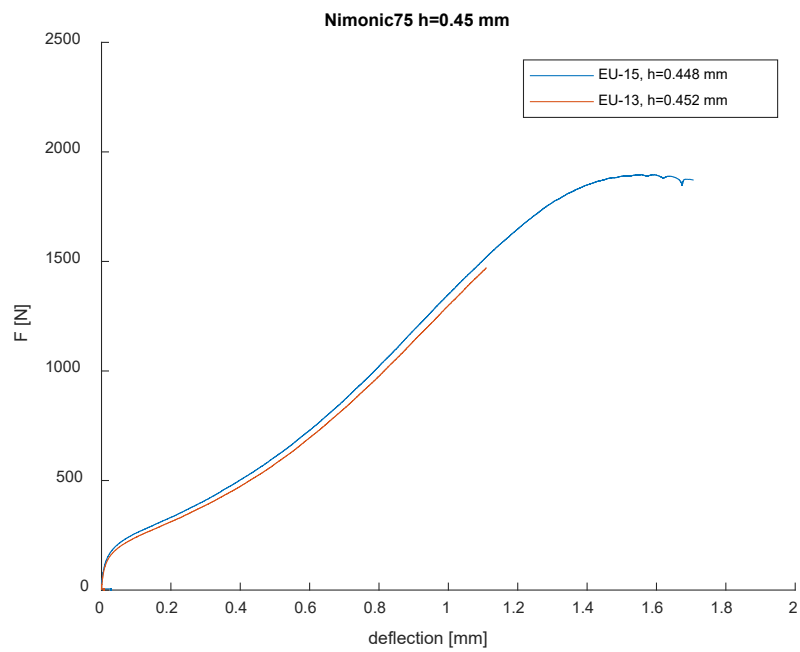


**Figure 8. Force-Deflection (F-u) curves for full and interrupted test with test piece thickness within  $0.45 \pm 0.05$  mm.**

## 4 FEA simulations

### 4.1 Constitutive law

Young modulus  $E$ , yield  $R_{p02}$ , ultimate tensile strength (UTS)  $R_m$ , and total elongation  $A$  for the NBCR-661 specific material batch of Nimonic 75 are summarised in Table 4 [7].

**Table 4. Material properties of the Nimonic 75 (BCR-661) [7].**

E [MPa]	$R_{p02}$ [MPa]	$R_m$ [MPa]	A [%]
206000	300	750	40.9

Uniaxial stress-strain data for the BCR-661 Nimonic 75 was found in [23].  $R_m$  value, obtained from Fig. 3 in [23] was slightly higher, 759 MPa, compared with Table 4 but still within the  $\pm 14$  MPa uncertainty, see Table 2.

For the uniaxial plastic stress-strain relationships, two analytical models were considered: a Ramberg Osgood and Voce. The Ramberg Osgood model is defined with Eq. (1). The value  $n$  is defined with Eq. (2) where points 1 and 2 refer to true values of stress and strain at  $R_{p02}$  and  $R_m$ , respectively. With such  $n$  value,  $k$  can be determined using the Eq. (3). The Voce model is defined with Eq. (4).

$$\varepsilon_{true} = \frac{\sigma_{true}}{E} + k \cdot \left(\frac{\sigma_{true}}{E}\right)^n \quad (1)$$

$$n = \frac{\log\left(\frac{E \cdot \varepsilon_1 - \sigma_1}{E \cdot \varepsilon_2 - \sigma_2}\right)}{\log\left(\frac{\sigma_1}{\sigma_2}\right)} \quad (2)$$

$$k = \frac{\frac{E \cdot \varepsilon_2}{\sigma_2}}{\left(\frac{\sigma_2}{E}\right)^n} \quad (3)$$

$$\sigma_{true} = R_0 + H \cdot \varepsilon_{pl} + Q \cdot (1 - e^{-b \cdot \varepsilon_{pl}}) \quad (4)$$

The comparison of the engineering values of the two models with the experimental data (digitized data from Fig 3 in [23]) shows a better agreement for the Voce model, Figure 9. Furthermore, the true stress levels off for large values of true strain for the Voce model, while for the Ramberg Osgood true stress keeps on increasing. The Voce model is therefore deemed more suitable to describe the stress/strain relationship for Nimonic 75 (BCR-661) and is therefore used from this point onwards for all FEA simulations.

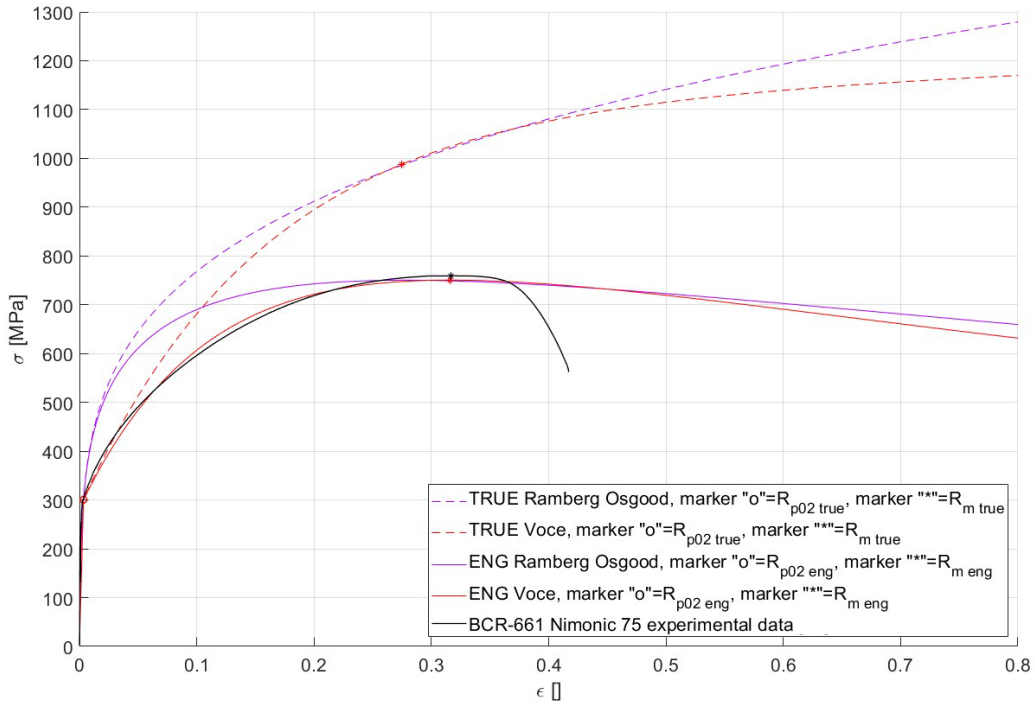


**Figure 9. Comparison of Ramberg Osgood and Voce analytical models with the Nimonic 75 (BCR-661) experimental data [23].**

Reference values, Table 4, are used for determining the parameters of Voce analytical model.  $R_0$  in Eq. (4) is assumed to be equal to true value of the yield stress, while the parameters  $H$ ,  $Q$ , and  $b$  are determined by solving a system of three equations:

- The first equation is obtained by applying the Voce expression to the true value of the  $R_m$  and the corresponding value of plastic strain at  $R_m$ .
- The second equation is based on the Considère necking criterion, stating that the onset of necking occurs when an increase in the (local) strain does result in increase in the load, Eqs. (5) and (6). Eq. (6) is therefore the second equation.
- The third equation is based on the relationship between true values and engineering values for the  $R_m$ , Eq. (7). It must be emphasized that the third equation is valid only until the UTS.

$$\Delta F = 0 \rightarrow F = A \cdot \sigma_{true} \rightarrow dF = 0 = dA \cdot \sigma_{true} + A \cdot d\sigma_{true} \quad (5)$$

$$\frac{d\sigma_{true}}{\sigma_{true}} = \frac{dA}{A} = d\varepsilon_{true} \rightarrow \sigma_{true} = \frac{d\sigma_{true}}{d\varepsilon_{true}} \quad (6)$$

$$R_m = \frac{\sigma_{Rm}}{1 + A_g} = \frac{\sigma_{Rm}}{\exp\left(\varepsilon_p Rm + \frac{\sigma_{Rm}}{E}\right)} \quad (7)$$

The parameters for the Voce expression are listed in Table 5.

**Table 5. Parameters of Voce expression for Nimonic 75 (BCR-661).**

$R_0$ [MPa]	$H$ [MPa]	$Q$ [MPa]	$b$
301.04	89.26	802.34	6.44

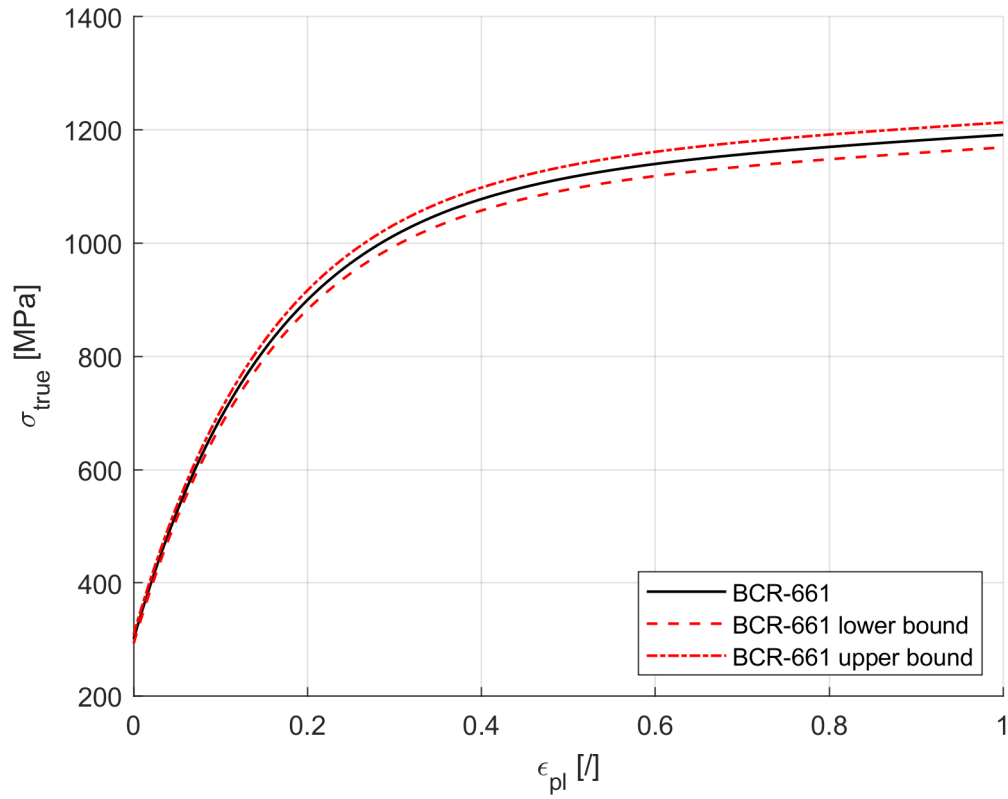


**Figure 10. Nimonic 75 (BCR-661) stress-strain curves. The lower/upper bounds are determined using uncertainty of 8 and 14 MPa for the proof,  $R_{p0.2}$ , and the tensile strength,  $R_m$ , c.f. Table 2.**

## 4.2 FEA model

A 2D axisymmetric FEA model as described in [24] is used to model Small Punch Tensile test in this work. The model has been validated for 316L, P91, P92, and 15-15Ti material [24]. ABAQUS finite element software is used [25].

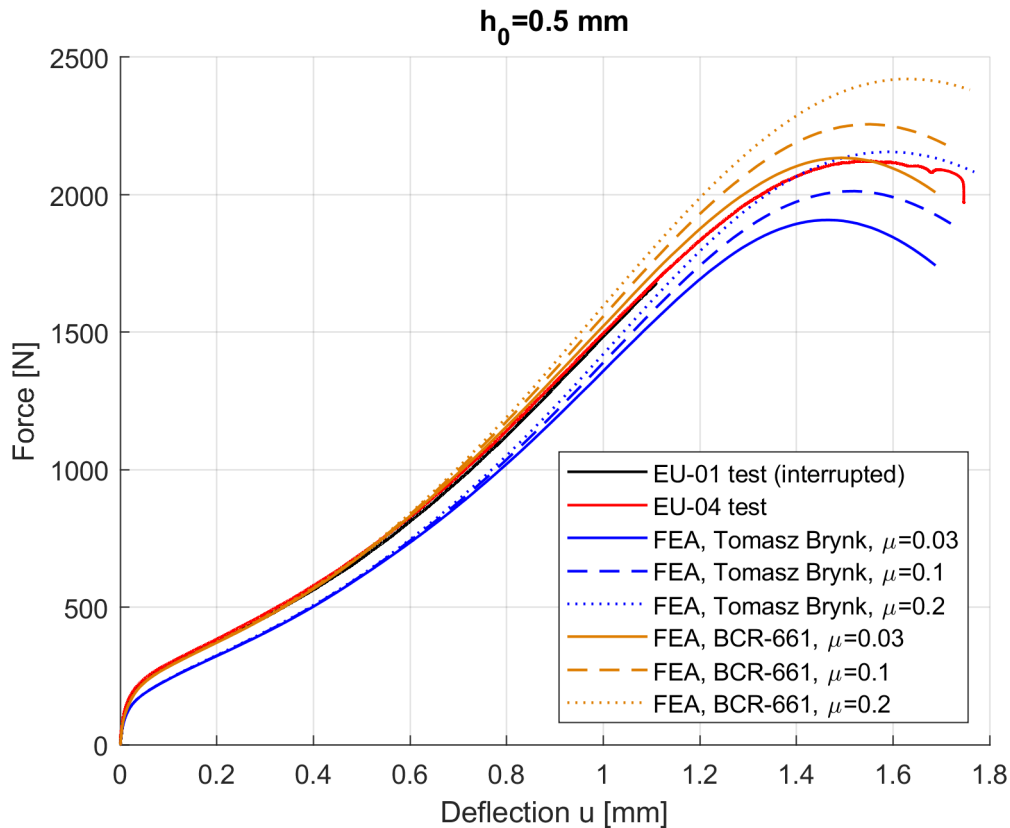


**Figure 11. FEA calculated Force-Deflection (F-u) compared to the experimental results.**

The FEA calculations result in practically the same force-deflection curve as the experimental data-up to the point where friction coefficient starts to affect the results (about 0.7, 0.8 mm of deflection). With the friction coefficient of  $\mu=0.03$ , the FEA results match the experimental ones well. However, it is clear that the friction coefficient of  $\mu=0.03$  seems unrealistically low. In literature, a friction coefficient between 0.1 and 0.3 have been reported. However, applying larger friction coefficients lead to an overestimation of the maximal force. It is foreseen that by introducing damage in the FEA analysis a decrease in the maximal force would follow. However, such work is out of scope within this project and is left for future work. These findings complicate the direct determination of the laboratory specific friction coefficient by test to simulation comparisons, which was a key objective of these experiments.

From this point onwards the Nimonic 75 (BCR-661) stress-strain curves used in FEA is that of Table 5. The proof,  $R_{p0.2}$ , and the tensile strength,  $R_m$ , have an uncertainty of 8 and 14 MPa, c.f. Table 2. Lower and upper bound of uniaxial stress-strain curves were therefore generated using the same procedure as explained above for Voce expression but using:

- $R_{p0.2}=300-8=292$  MPa and  $R_m=750-14=736$  MPa  $\rightarrow$  Nimonic 75 (BCR-661) lower bound strain-stress curve.
- $R_{p0.2}=300+8=308$  MPa and  $R_m=750+14=764$  MPa  $\rightarrow$  Nimonic 75 (BCR-661) upper bound strain-stress curve.

The corresponding small punch tensile force-deflection curves, Figure 12 and Table 6, deviate negligibly from the ones, calculated using the nominal Nimonic 75 (BCR-661) certified values,  $R_{p0.2}=300$  MPa and  $R_m=750$  MPa, Table 6.

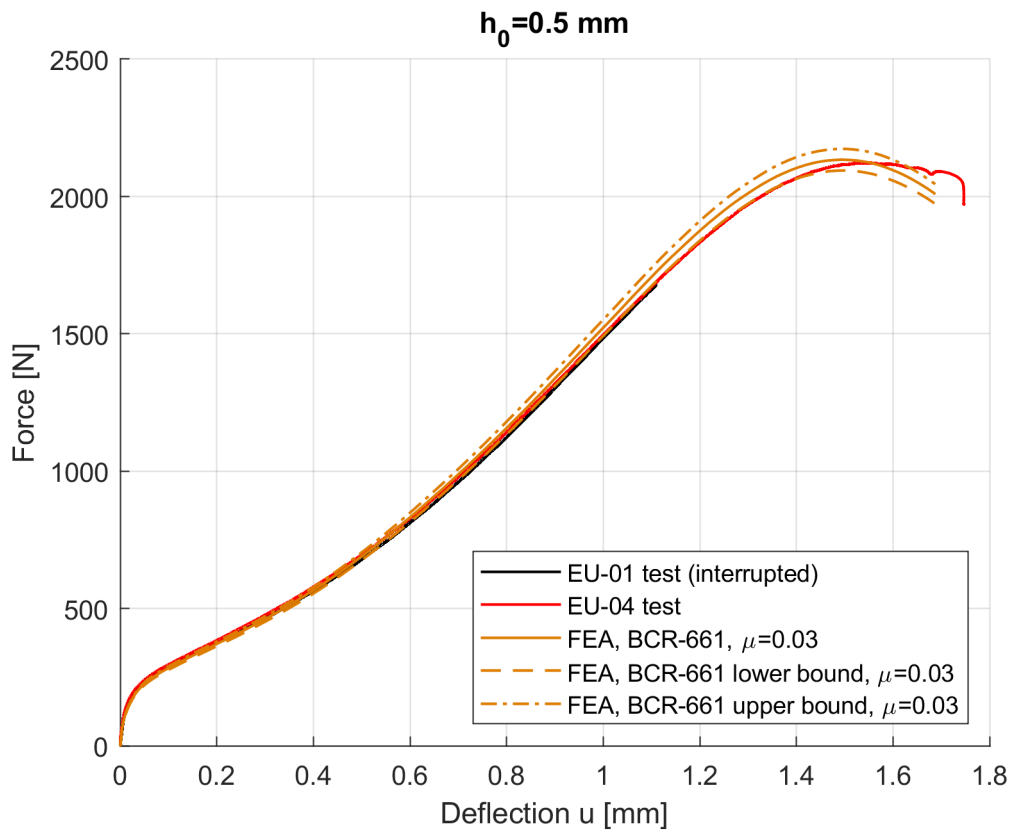


**Figure 12. Effect of using Nimonic 75 (BCR-661) lower and upper bound uniaxial tensile properties on FEA Force-Deflection (F-u) curves.**

**Table 6. Effect on Nimonic 75 (BCR-661) lower and upper bounds on  $F_m$ .**

Friction coefficient $\mu$	$F_m$ BCR-661 lower bound [N]	$F_m$ BCR-661 [N]	$F_m$ BCR-661 upper bound [N]
0.03	2094.5	2134.0	2173.1
0.1	2214.4	2256.1	2297.6
0.2	2376.1	2420.8	2465.3

Only the Nimonic 75 (BCR-661) nominal values with the properties listed in Table 5 ( $R_{p0.2}=300 \text{ MPa}$  and  $R_m=750 \text{ MPa}$ ) are used from this point onwards.

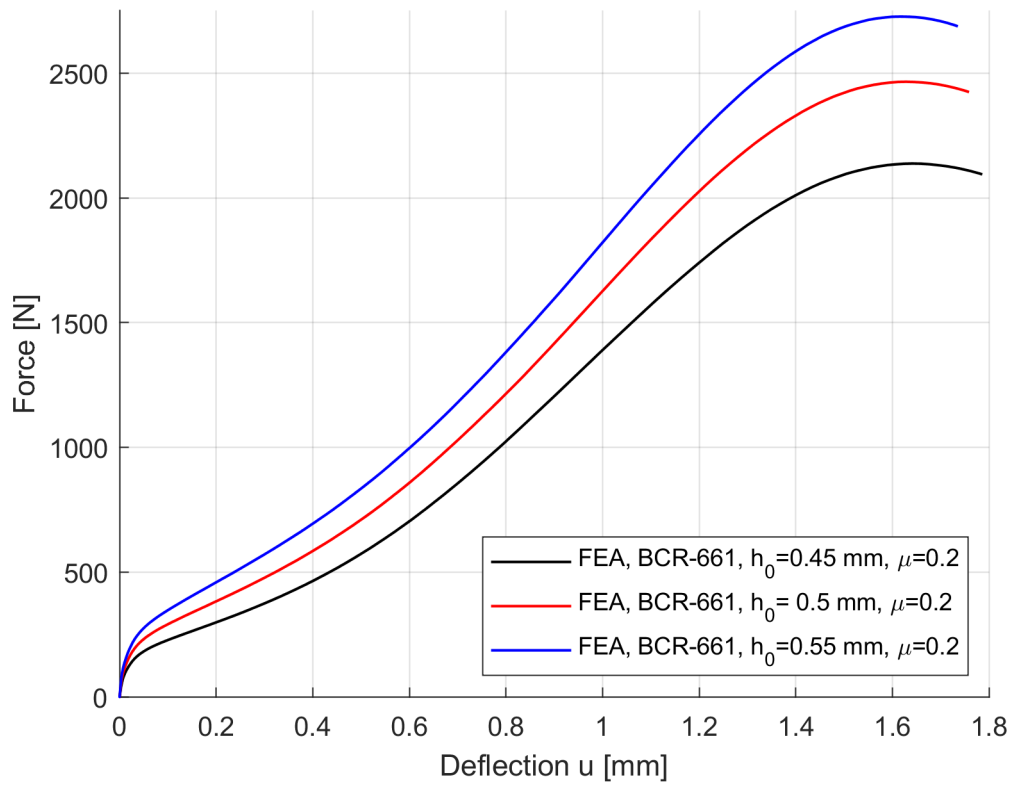


**Figure 13. FEA simulated Force-Deflection (F-u) curves for test piece thicknesses of 0.45, 0.50 and 0.55 mm with a 0.2 friction coefficient applied.**

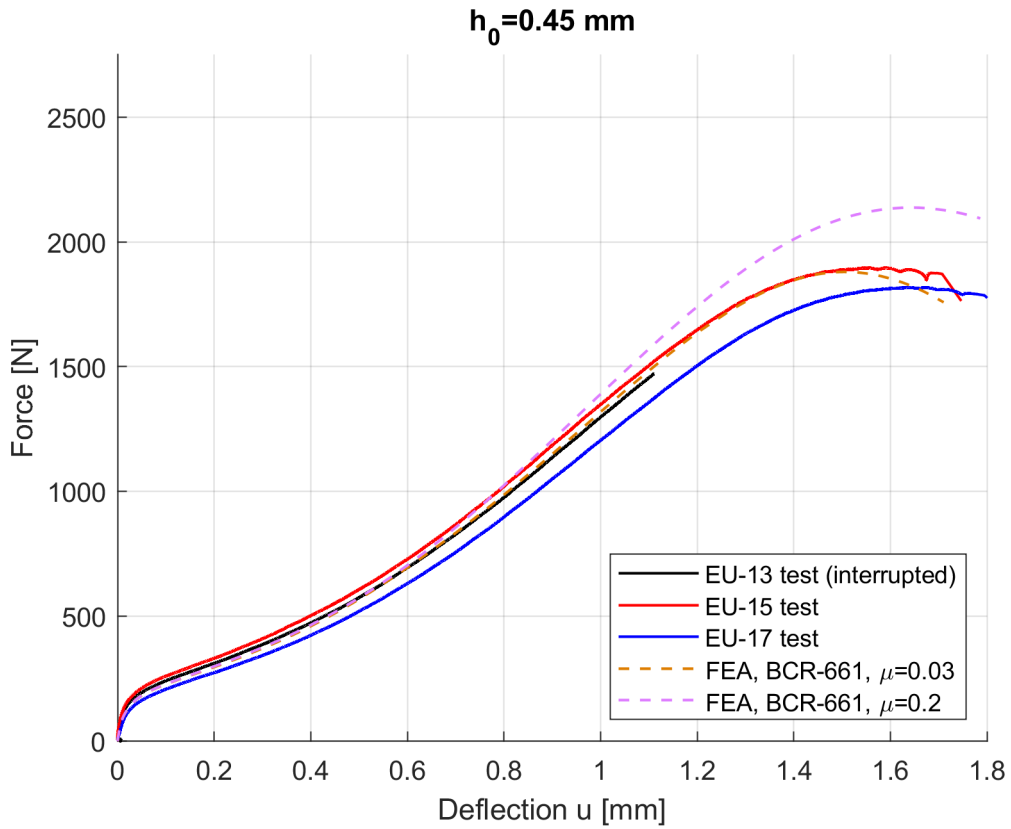


**Figure 14. Comparison of experimental and FEA results for test piece thickness of 0.45 mm.**

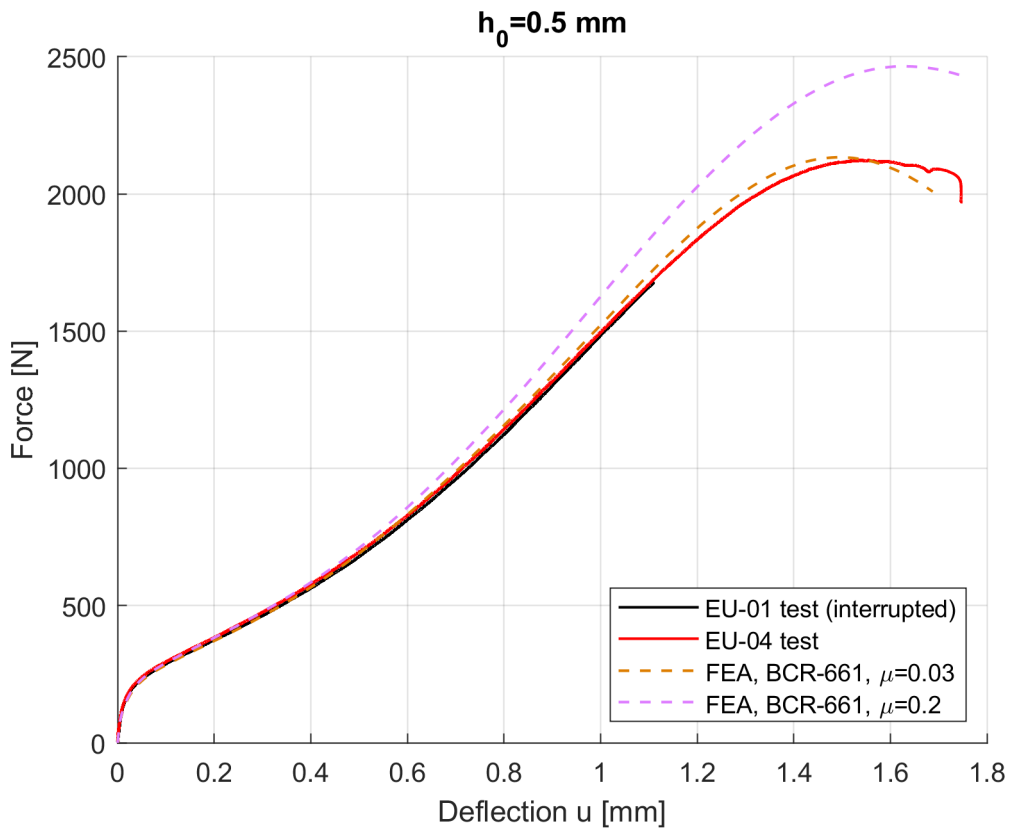


**Figure 15. Comparison of experimental and FEA results for test piece thickness of 0.5 mm.**

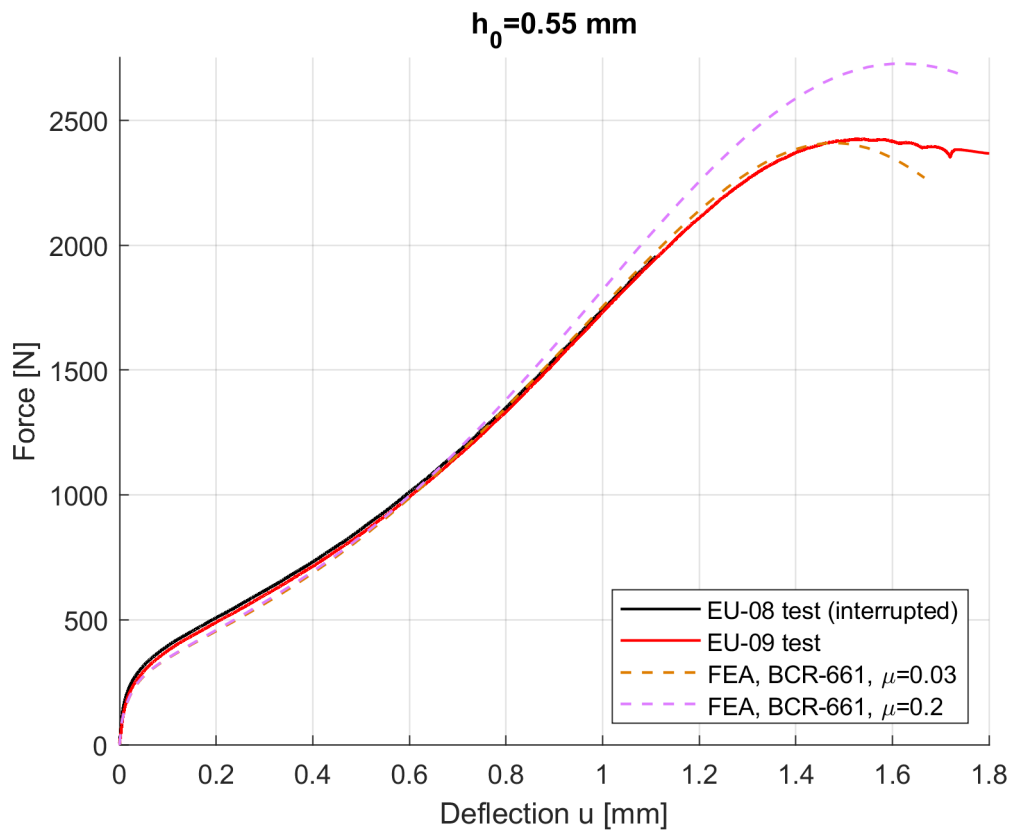


**Figure 16. Comparison of experimental and FEA results for test piece thickness of 0.55 mm.**

These simulation curves are later used for comparison to the actual test curves in the assessment part of this report.

## 5 Test data assessment for proof and tensile strength

Differences between laboratories using different types of punchers, e.g. hemispherical punchers made from high temperature resistant Ni-based alloys (e.g. Nimonic 90) or ceramic bearing balls ( $\text{Si}_3\text{N}_4$ ) can affect the SP tensile strength estimates, e.g. due to small differences in friction between the test piece and the punch and/or differences in the final force-displacement curve behaviour after reaching a displacement with full hemispherical area contact. The test set-up differences potentially impact the measured maximum force ( $F_m$ ) and the deflection at maximum force ( $u_m$ ) of the force-deflection curve, Eq. (8). The test piece thickness will naturally have an effect on the acquired level of  $F_m$ , but both FEA simulations and the Chakrabarty membrane stretch theory [26] show that  $u_m$  is nearly unaffected by thickness differences in the magnitude used here. Thus, indicating that the classical equation for tensile strength, Eq. (8) below, will be affected by the two studied variables, i.e. thickness and friction. These differences are to be considered also for the estimation of proof strength. A future inter-laboratory round-robin based on the preliminary results of this report is currently being planned, and the outcome is hoped to support the further development of the test methodology itself and the force-to-stress correlations for tensile and proof strength. It is also to be noted that when using displacement as a measure (instead of deflection), there is the additional impact of machine compliance that will further increase the uncertainty of the estimation.

$$R_m = \alpha \cdot \frac{F_m}{h_0 \cdot u_m \text{ (or } v_m)} \quad (8)$$

$$R_p = \beta \cdot \frac{F_e}{h_0^2} \quad (9)$$

$$E_{fl} = \int_0^{u_B} F(u) du \quad (10)$$

$$F_{fl} = \frac{E_{fl}}{u_B} \quad (11)$$

$$R_p = \beta_{fl} \cdot \frac{F_{fl}}{h_0^2} \quad (12)$$

The estimation of the ultimate tensile strength,  $R_m'$ , is classically performed by extracting the maximum force  $F_m$  of the curve and dividing it with the product of the initial thickness and the deflection  $u_m$  (or displacement  $v_m$ ) at the location of  $F_m$ , see Eq. (8).

The estimation of the uniaxial engineering proof stress,  $R_p'$ , is classically based on the assumption that the force in the initial stage of the tests can be correlated to an extracted force  $F_e$  divided by the square of the initial test piece thickness  $h_0$ , see Eq. (9). Here the Eq. (9) methodology is assessed with three optional methods, i.e. the standard tri-linear method, the offset method and a method based on a characteristic 'flow force'  $F_{fl}$  represented by the plastic energy ( $E_{fl}$ ) between zero and  $u_B=0.5$  mm (also the pivot point on the SP curve for the tri-linear  $F_e$  determination) divided by the deflection  $u_B$ , as given in Eqs. (10)-(12). The plastic energy is also used for determining the ductile to brittle transition temperature by SP testing in the EN 10371 standard.

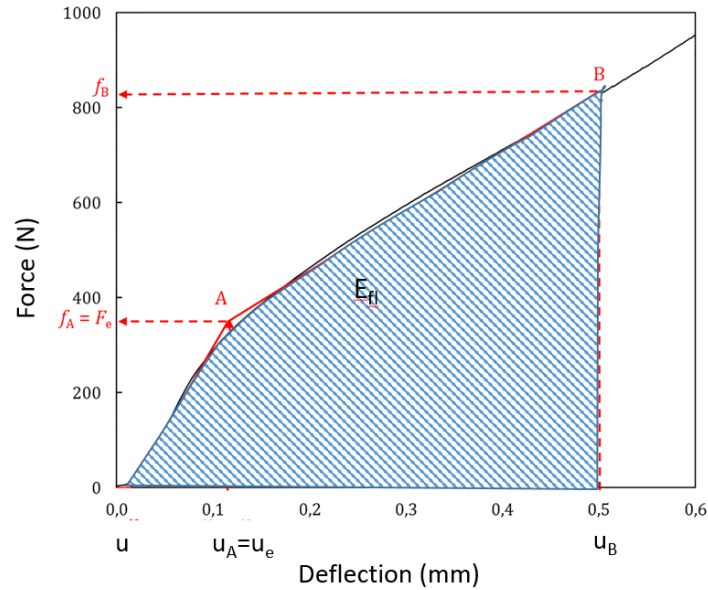


**Figure 17. Tri-linear method (standard EN 10371) for extracting  $F_e$  and the surface  $E_{fi}$  that gives  $F_{fi}$  when divided by  $u_B$ .**

Some of the challenges arising in the estimation of tensile properties are well known, for instance the force-to stress parameter  $\beta$  for proof strength estimation, Eq. (9), is affected by strain hardening. The here presented models based on plastic energy is also affected by strain hardening behaviour, but might be less sensitive to small differences in the initial part of the force-deflection curve. As such, the  $F_{fi}$  forces, Eqs. (10) and (11), could potentially be used to determine a ‘flow stress’ that could be further correlated to  $R_p$ , e.g.  $R_p = f(R_m, R_{fi})$ . One of the main challenges in extracting classical values of  $F_e$ , Figure 17, in a repeatable robust way, is that the raw data frequently needs pre-processing, e.g. deciding on how to cull the data in the very beginning of the test curve. In the case of the offset method again, the data range for the slope needs to be defined, making the extracted value dependent on the assessor’s choice. Using the plastic energy based  $F_{fi}$  would as such have the benefit of removing most of the assessor dependent data processing.

## 6 Test results and SP correlation parameters based on the reference material verified tensile properties

The results from extracting the  $u_m$ ,  $F_m$  and  $F_e$  values from the SP test curves are presented in Table 7. Note that the  $F_e$  – EN10371 is the current EN standard assessment method, the  $F_e$ -proj (projection) is the method used in ASTM code (3205-20-ASTM) [27]. The  $F_e$ -offs (offset) is extracted from the data by an offset of 0.01 times the test piece thickness on the slope given by the initial force-deflection data range 30-100 N. Starting at 30 N on the curve avoids the inconsistencies sometimes present at the very low forces, potentially caused by punch / ball settling. The test by test solved correlation constants, calculated from the verified proof stress of 300 MPa and tensile strength 750 MPa by rearranging Eq. (9), are shown in Figure 18 for the different proof strength  $F_e$  extraction methods and in Figure 19 for the tensile strength methods by rearranging Eq. (8). In Figure 18 the new method of using  $F_{fl}$  for predicting the proof strength is also given.

**Table 7. Extracted  $u_m$ ,  $F_m$  and  $F_e$  (u) values from the test data.**

ID code	$h_0$ (mm)	$u_m$ (mm)	$F_m$ (N)	$F_e$ EN10371 (N)	$F_e$ -proj (N)	$F_e$ -offs. $h/10$ (N)	$F_{fl}$ (N)	Note
EU-17	0.431	1.634	1818	131	114	189	309	Full test, higher $u_m$ than others [8]
EU-15	0.448	1.557	1896	171	146	230	374	Full test [9]
EU-06	0.485	1.563	2037	186	157	242	397	Full test [10]
EU-04	0.498	1.531	2123	201	163	258	426	Full test [11]
EU-07	0.523	1.532	2328	243	189	300	510	Full test [12]
EU-09	0.556	1.537	2426	278	227	322	536	Full test [13]
EU-13	0.452	N/A	N/A	153	126	211	351	Interrupted [14]
EU-01	0.501	N/A	N/A	187	156	251	420	Interrupted [15]
EU-08	0.557	N/A	N/A	286	225	335	555	Interrupted [16]

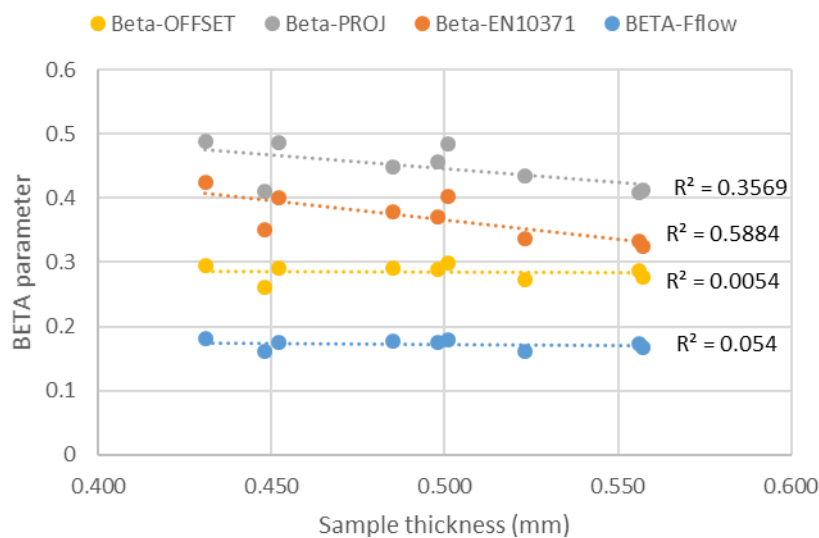


**Figure 18. Test specific optimal  $\beta$  parameters, calculated to acquire a  $R_p$  of 300 MPa, see Eq. (9), as a function of test piece thickness. The  $\beta$  parameter is based on the  $h/10$  offset.**

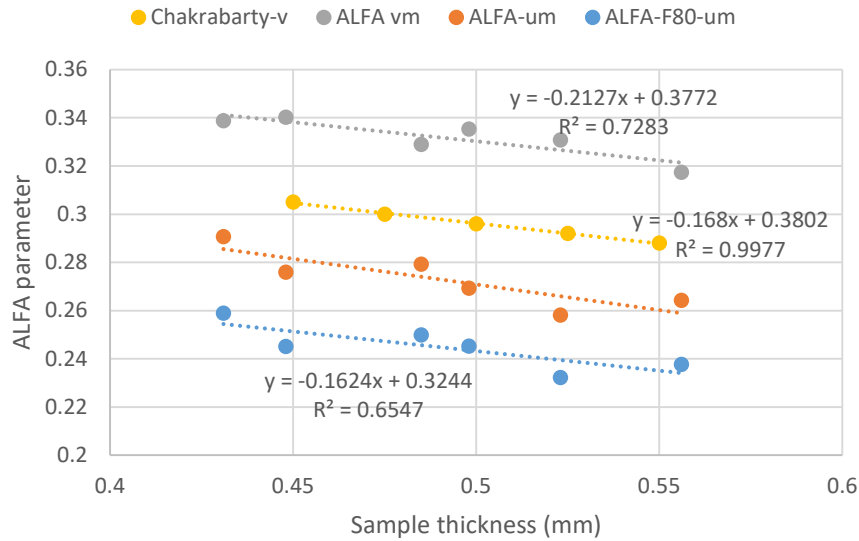


**Figure 19. Test specific optimal  $\alpha$  parameters, calculated to acquire a  $R_m$  of 750 MPa, see Eq. (8), as a function of test piece thickness. Note that the Chakrabarty based evaluation of the parameter indicates the same slope as found for the measured test results.**

It can be noted that for proof strength estimation the methods currently used in standards are in all cases somewhat thickness dependent whereas the offset method and the flow force methods seemingly are thickness independent.

For the tensile strength estimation all attempted estimations were thickness dependent, with slopes predictable with the Chakrabarty membrane stretching equations [26].

**Table 8. Extracted  $u_m$ ,  $F_m$  and  $F_e$  values from the simulated data.**

ID code	$h_0$ (mm)	$u_m$ (mm)	$F_m$ (N)	$F_e$ (N)
045- $\mu=0.03$	0.450	1.504	1880	93.9
050- $\mu=0.03$	0.500	1.493	2134	114
055- $\mu=0.03$	0.550	1.478	2409	155.6
045- $\mu=0.1$	0.450	1.563	1989	92.4
050- $\mu=0.1$	0.500	1.552	2298	126.3
055- $\mu=0.1$	0.550	1.534	2544	141.8
045- $\mu=0.2$	0.450	1.641	2138	95.2
050- $\mu=0.2$	0.500	1.628	2465	119.7
055- $\mu=0.2$	0.550	1.615	2727	150.5
045- $\mu=0.3$	0.450	1.682	2249	93.3
050- $\mu=0.3$	0.500	1.687	2555	112.7
055- $\mu=0.3$	0.550	1.691	2879	150

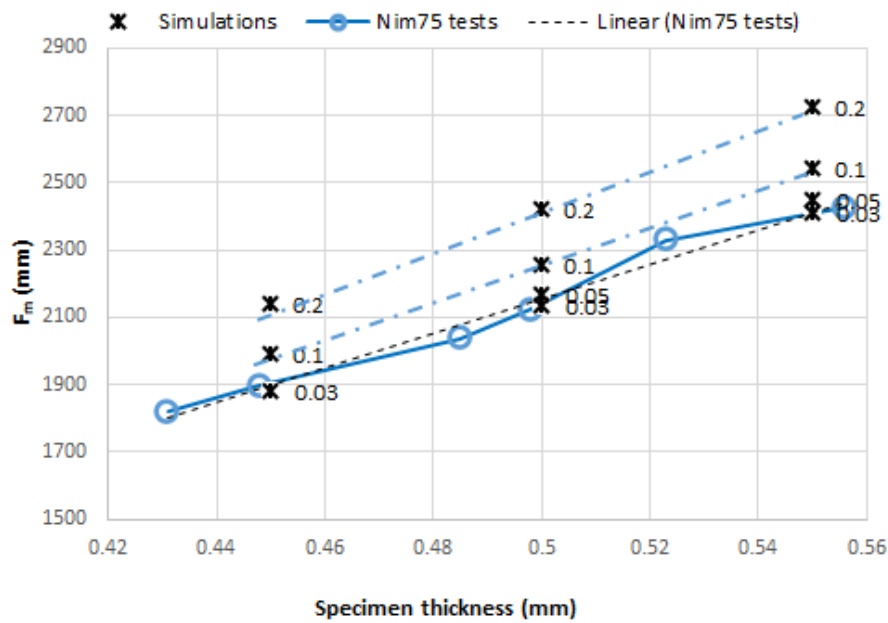


Figure 20. Variation of  $F_m$  in FEA simulations ( $\mu=0.03-0.2$ ) as a function of test piece thickness in comparison to SP tests.

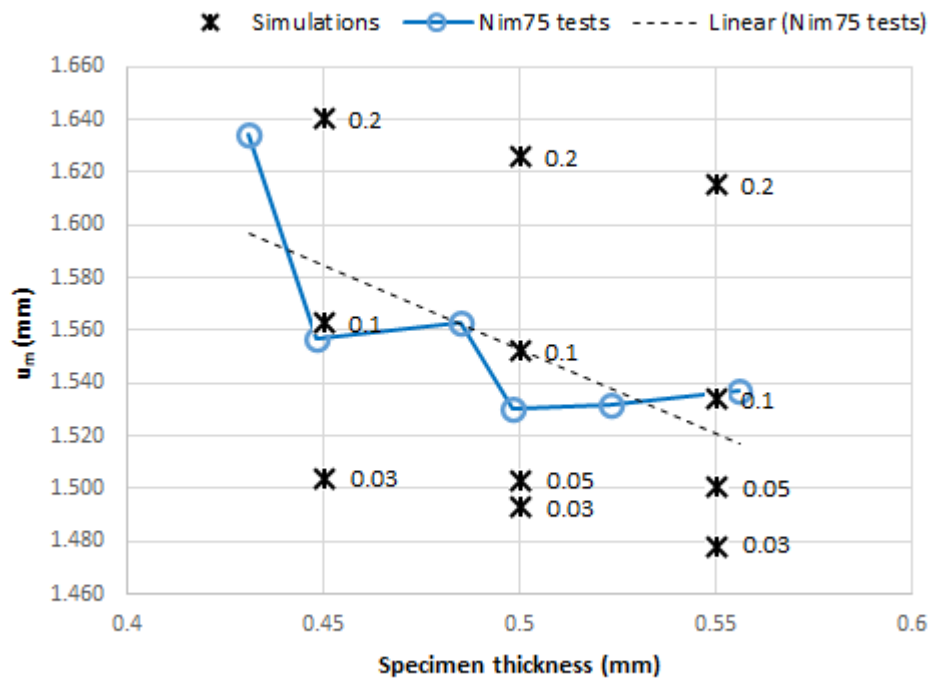
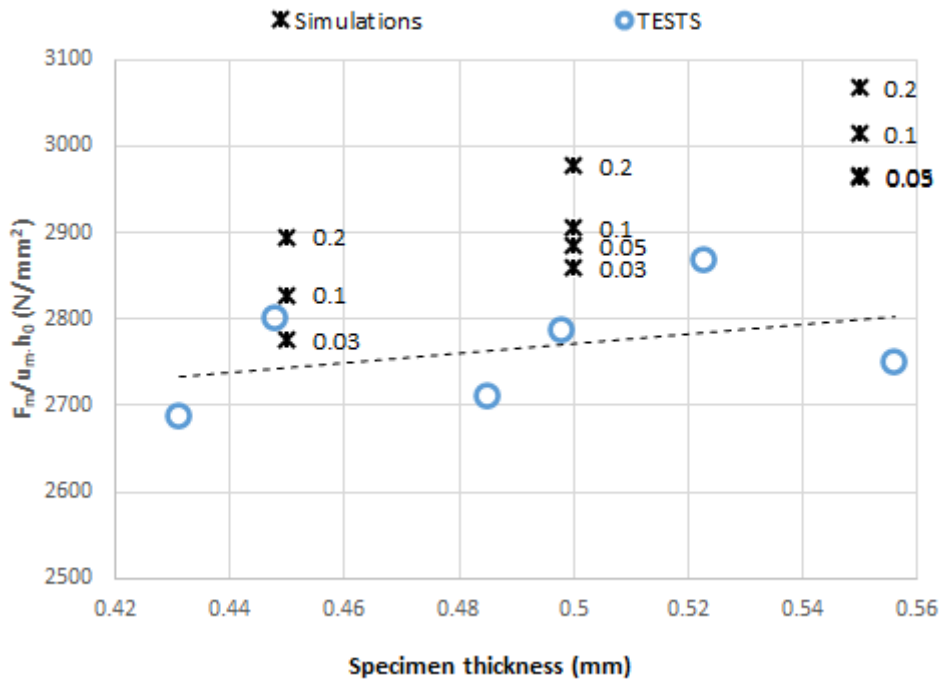


Figure 21. Variation of  $u_m$  in FEA simulations ( $\mu=0.03-0.3$ ) as a function of test piece thickness in comparison to SP test results.



**Figure 22. Thickness dependence of the classical formulation  $R_m$  correlation, Eq. (8), between FEA simulations (Nimonic 75 (BCR-661) with  $\mu=0.03-0.2$ ) and tests.**

It can be seen from Figure 20 and Figure 21 that the  $F_m$  is dependent on the thickness whereas the  $u_m$  is nearly thickness independent. The same result is acquired using the Chakrabarty membrane stretching equations (which assume  $\mu=0$ ), showing that the deflection in the location where the maximum Force over stress value is acquired is constant for a specific tests setup (same puncher radius and receiving hole). The error in estimating the  $R_m$  for the same material, here Nimonic 75 (BCR-661), could be up to 8% (the linear relationship in Figure 22), if the same  $\alpha$  parameter is used for specimen of the test piece thicknesses of 0.45 and 0.55 mm. In Table 9 the optimal  $\alpha$  for the standard  $F_m-u_m$ , Eq. (8), procedure (giving an average estimate of the true reference material  $R_m$ ) is given for Nimonic 75 (BCR-661) together with a similar estimate using the force at 80% of the maximum ( $F_{80\%}$ ) and the deflection at this force ( $u_{80\%}$ ) in an attempt to minimize the impact of friction.

As a consequence of these findings the extraction of tensile strength estimates from SP tests (see Figure 22) using a constant  $\alpha$  parameter, Eq. (8), between alloys with different hardening behaviour should be studied further and high precision on test pieces thicknesses should be required. Alternatively, corrections needs to be applied on the  $\alpha$  parameter as a function of thickness and preferably also on the lab specific friction coefficient.

**Table 9. Comparison of two  $R_m$  estimation methods, the  $\alpha$  constant given in the informative annex C of EN 10371 is 0.278 (from data mainly including Ferritic/Martensitic steels with a  $R_{p0.2}/R_m$  ratio in the range of 80%).**

Based on	$F_m$	$F_{80\%}$	Note
Average constant $\alpha$	0.272	0.245	The $F_m$ -EN10371 Annex C of $\alpha= 0.278$ (for $F_m$ ) is compliant with the here evaluated result
1 Standard deviation of estimate $R_m$ – all thicknesses	4.2%	3.8%	Both using the $F_m - u_m$ and $F_{80\%} - u_{80\%}$ give very similar results → friction influence negligible since it is 'equal' between tests

**Table 10. Comparison of four  $R_p$  estimation methods, the  $\beta$  constant given in the informative annex D of EN 10371 is 0.510 (from data mainly including Ferritic/Martensitic steels with a  $R_{p0.2}/R_m$  ratio in the range of 80%).**

Based on	$F_e - EN10371$ (N)	$F_e$ -proj (N)	$F_e$ -offs. (N)	$F_{rl}$ (N)	Note
Average constant $\beta$	0.356	0.448	0.285	0.172	The $F_e$ -EN10371 of Annex D, $\beta= 0.479$ , is clearly deviating from the here evaluated result. The unsolved deviance found between FEA and test curves could be linked.
1 Standard deviation of $\beta$ – all thicknesses	3.5%	3.3%	1.2%	0.7%	The $F_e$ -offset and $F_{rl}$ methods are the best performing → the trilinear methods extraction causes the largest scatter

## 7 Conclusion

SPT at RT for Nimonic 75 (BCR-661) reference material has been assessed for determining the sensitivity of the miniature test to capture the certified uniaxial material properties. Using a set of different test piece thicknesses in the range 0.45 to 0.55 mm it was possible to estimate the specific test facility friction for the E3000 small punch test set-up at the JRC Petten SMPA lab. It has been shown that the classical correlation methods based on specific extracted forces and deflections (or displacements) are sensitive to test piece thickness and a constant value of the correlation factors is not sufficient in the thickness range investigated. The material test results have successfully been used for determining a test-facility specific friction coefficient. The results of this assessment and this report can be utilized for further planning of the planned interlaboratory round-robin.

These results are planned to be published in scientific journal in the near future. The data generated for the reference material is made available in the JRC data base MATDB [8] to [22] and in catalogue format in [28].

For the planned future interlaboratory round robin the following aspects of small punch testing should be emphasized and required to be present in the reporting by each participating testing laboratory:

- Detailed description of the testing machine, load cell capacity and type of deformation measurement (load-line displacement  $w$ , displacement  $v$  or deflection  $u$ ).
- Test specifics, e.g. ball / puncher type, receiving hole, chamfer type, compliance correction method, etc. reported as measured values (not nominal) where applicable.
- The actual test piece thickness (5 positions) measured.
- Data to be provided in unaltered raw data form and in edited / 'processed' from that is used to extract specific assessor / lab specific forces and deformations.

It is however important to remember that the planned round-robin is targeting to establish a qualified **test response** to verify the test equipment and not specifically to solve the challenges remaining on the material property estimation.

**Glossary, abbreviations and definitions as given in [4].**

<b>Symbol</b>	<b>Unit</b>	<b>Designation</b>
$A_{gt}$	%	Total uniform elongation of the uniaxial tensile test
$\alpha$	-	Force to stress correlation factor for estimation of $R_m$
$\beta$	-	Force to stress correlation factor for estimation of $R_p$
$C_p$	mm/N	Compliance of punch and push rod
$d$	mm	Diameter of the punch tip
$D$	mm	Diameter of the receiving hole (lower die)
$D_s$	mm	Diameter of the test piece
$E_Y$	GPa	Young's modulus
$\varepsilon_f$	-	Effective fracture strain $\varepsilon_f = \ln(h_0/h_f)$
$F$	N	Force applied to the specimen
$F_e$	N	Elastic-plastic transition force in a small punch test
$F_m$	N	Maximum of $F$ during the test
$h$	mm	Thickness of the test piece
$h_0$	mm	Initial thickness of test piece (e.g. before corrosion exposure)
$h_f$	mm	Measured wall thickness at failure (here before final collapse / punch through)
$h_e$	mm	Estimated 'effective' thickness of the test piece
$L$	mm	Length of the chamfer in the receiving hole
$\Psi$	N/MPa	Force to stress ratio used in Chakrabarty membrane stretch equations
$R_m$	MPa	Ultimate tensile strength
$R_p$	MPa	Proof strength
$R_f$	MPa	Flow stress (e.g. average of proof and tensile strength)
$\sigma$	MPa	Equivalent stress
$T$	°C, K	Test temperature
$u$	mm	Deflection of the specimen measured from below test piece
$u_e$	mm	Deflection at $F_e$

<b>Symbol</b>	<b>Unit</b>	<b>Designation</b>
$u_m$	mm	Deflection at $F_m$
$v$	mm	Displacement of the ball/punch tip
$v_r$	mm	Displacement at rupture
$w$	mm	Displacement of the crosshead

## List of figures

Figure 1. Test piece extraction from Nimonic 75 (BCR-661) rod. ....	7
Figure 2. Nimonic 75 (BCR-661) test piece thicknesses, blue test pieces used for full tests, yellow for interrupted tests. ....	8
Figure 3. Force-Deflection (F-u) curves at room temperature for the different test piece thicknesses. ....	9
Figure 4. Force-Deflection (F-u) curves at 450°C for the different test piece thicknesses [17], [18], [19], [20], [21], and [22]. ....	9
Figure 5. Full 3D surface scan for Nimonic 75 (BCR-661) test piece. The 3D profilometer measured deflection $u_{meas} = 1.080$ mm for the interrupted test and 1.624 mm for the full test. The corresponding LVDT measure values are 1.11 and 1.74 mm correspondingly. ....	10
Figure 6. Force-Deflection (F-u) curves for full and interrupted test with test piece thickness within $0.5 \pm 0.05$ mm. ....	10
Figure 7. Force-Deflection (F-u) curves for full and interrupted test with test piece thickness within $0.56 \pm 0.05$ mm. ....	11
Figure 8. Force-Deflection (F-u) curves for full and interrupted test with test piece thickness within $0.45 \pm 0.05$ mm. ....	11
Figure 9. Comparison of Ramberg Osgood and Voce analytical models with the Nimonic 75 (BCR-661) experimental data [23]. ....	13
Figure 10. Nimonic 75 (BCR-661) stress-strain curves. The lower/upper bounds are determined using uncertainty of 8 and 14 MPa for the proof, $R_{p0.2}$ , and the tensile strength, $R_m$ , c.f. Table 2. ....	14
Figure 11. FEA calculated Force-Deflection (F-u) compared to the experimental results. ....	15
Figure 12. Effect of using Nimonic 75 (BCR-661) lower and upper bound uniaxial tensile properties on FEA Force-Deflection (F-u) curves. ....	16
Figure 13. FEA simulated Force-Deflection (F-u) curves for test piece thicknesses of 0.45, 0.50 and 0.55 mm with a 0.2 friction coefficient applied. ....	17
Figure 14. Comparison of experimental and FEA results for test piece thickness of 0.45 mm. ....	18
Figure 15. Comparison of experimental and FEA results for test piece thickness of 0.5 mm. ....	18
Figure 16. Comparison of experimental and FEA results for test piece thickness of 0.55 mm. ....	19
Figure 17. Tri-linear method (standard EN 10371) for extracting $F_e$ and the surface $E_{fl}$ that gives $F_{fl}$ when divided by $u_B$ . ....	21
Figure 18. Test specific optimal $\beta$ parameters, calculated to acquire a $R_p$ of 300 MPa, see Eq. (9), as a function of test piece thickness. The $\beta$ parameter is based on the h/10 offset. ....	22
Figure 19. Test specific optimal $\alpha$ parameters, calculated to acquire a $R_m$ of 750 MPa, see Eq. (8), as a function of test piece thickness. Note that the Chakrabarty based evaluation of the parameter indicates the same slope as found for the measured test results. ....	23
Figure 20. Variation of $F_m$ in FEA simulations ( $\mu=0.03-0.2$ ) as a function of test piece thickness in comparison to SP tests. ....	24
Figure 21. Variation of $u_m$ in FEA simulations ( $\mu=0.03-0.3$ ) as a function of test piece thickness in comparison to SP test results. ....	24
Figure 22. Thickness dependence of the classical formulation $R_m$ correlation, Eq. (8), between FEA simulations (Nimonic 75 (BCR-661) with $\mu=0.03-0.2$ ) and tests. ....	25

## List of tables

Table 1. Chemical analysis of 14 mm diameter reference material bars (mass %) as given in [5].	6
Table 2. Material properties according to the certificate of analysis [7].	6
Table 3. Test piece identification codes, ordered by measured thicknesses, the original measurement performed at SCK CEN with a 10 $\mu\text{m}$ resolution and re-measured at JRC with a 1 $\mu\text{m}$ resolution.	7
Table 4. Material properties of the Nimonic 75 (BCR-661) [7].	12
Table 5. Parameters of Voce expression for Nimonic 75 (BCR-661).	14
Table 6. Effect on Nimonic 75 (BCR-661) lower and upper bounds on $F_m$ .	16
Table 7. Extracted $u_m$ , $F_m$ and $F_e(u)$ values from the test data.	22
Table 8. Extracted $u_m$ , $F_m$ and $F_e$ values from the simulated data.	23
Table 9. Comparison of two $R_m$ estimation methods, the $\alpha$ constant given in the informative annex C of EN 10371 is 0.278 (from data mainly including Ferritic/Martensitic steels with a $R_{p0.2}/R_m$ ratio in the range of 80%).	26
Table 10. Comparison of four $R_p$ estimation methods, the $\beta$ constant given in the informative annex D of EN 10371 is 0.510 (from data mainly including Ferritic/Martensitic steels with a $R_{p0.2}/R_m$ ratio in the range of 80%).	26

## References

- [1] E. Altstadt, An Improved Correlation for the Estimation of the Yield Strength from Small Punch Testing, *Metals* 13(10) (2023), <https://doi.org/10.3390/met13101716>.
- [2] J.C. Chica, P.M.B. Díez, M.P. Calzada, Development of an improved prediction method for the yield strength of steel alloys in the Small Punch Test, *Mater. Des.* 148 (2018) 153-166, <https://doi.org/10.1016/j.matdes.2018.03.064>.
- [3] P. Hähner, C. Soyarslan, B.G. Çakan, S. Bargmann, Determining tensile yield, stresses from Small Punch tests: A numerical-based scheme, *Mater. Des.* 182 (2019), 107974, <https://doi.org/10.1016/j.matdes.2019.107974>.
- [4] EN 10371:2021, Metallic materials Small punch test method, European Standards.
- [5] Ingelbrecht C, Loveday M. The Certification of Tensile Properties of an Ambient Temperature Tensile Testing Reference Material According to EN10002-1, CRM 661. EUR 19589 EN. 2000. JRC20194 <https://publications.jrc.ec.europa.eu/repository/handle/JRC20194>.
- [6] Certified Reference Materials catalogue of the JRC, [BCR-661B NIMONIC 75 FOR TENSILE PROPERTIES](https://crm.jrc.ec.europa.eu/p/40456/40485/By-analyte-group/Mechanical-properties/BCR-661B-NIMONIC-75-FOR-TENSILE-PROPERTIES/BCR-661B), <https://crm.jrc.ec.europa.eu/p/40456/40485/By-analyte-group/Mechanical-properties/BCR-661B-NIMONIC-75-FOR-TENSILE-PROPERTIES/BCR-661B>.
- [7] Certified Reference Materials catalogue of the JRC, Certificate/Prod. Info. Sheet BCR-661 certificate.pdf, <https://crm.jrc.ec.europa.eu/p/40456/40485/By-analyte-group/Mechanical-properties/BCR-661B-NIMONIC-75-FOR-TENSILE-PROPERTIES/BCR-661B>.
- [8] Brynk, T.; Holmström, S. (2024): Small punch tensile/fracture test data for Nimonic 75 (BCR 661) material at 21 °C and a displacement rate of .00834 mm/s (specimen identifier EU-17), version 1.0, European Commission JRC, [Dataset], <https://doi.org/10.5290/180001>.
- [9] Brynk, T.; Holmström, S. (2024): Small punch tensile/fracture test data for Nimonic 75 (BCR 661) material at 21 °C and a displacement rate of .00834 mm/s (specimen identifier EU-15), version 1.0, European Commission JRC, [Dataset], <https://doi.org/10.5290/180002>.
- [10] Brynk, T.; Holmström, S. (2024): Small punch tensile/fracture test data for Nimonic 75 (BCR 661) material at 21 °C and a displacement rate of .00834 mm/s (specimen identifier EU-06), version 1.0, European Commission JRC, [Dataset], <https://doi.org/10.5290/180003>.
- [11] Brynk, T.; Holmström, S. (2024): Small punch tensile/fracture test data for Nimonic 75 (BCR 661) material at 21 °C and a displacement rate of .00834 mm/s (specimen identifier EU-04), version 1.0, European Commission JRC, [Dataset], <https://doi.org/10.5290/180004>.
- [12] Brynk, T.; Holmström, S. (2024): Small punch tensile/fracture test data for Nimonic 75 (BCR 661) material at 21 °C and a displacement rate of .00834 mm/s (specimen identifier EU-07), version 1.0, European Commission JRC, [Dataset], <https://doi.org/10.5290/180005>.
- [13] Brynk, T.; Holmström, S. (2024): Small punch tensile/fracture test data for Nimonic 75 (BCR 661) material at 21 °C and a displacement rate of .00834 mm/s (specimen identifier EU-09), version 1.0, European Commission JRC, [Dataset], <https://doi.org/10.5290/180006>.
- [14] Brynk, T.; Holmström, S. (2024): Small punch tensile/fracture test data for Nimonic 75 (BCR 661) material at 21 °C and a displacement rate of .00834 mm/s (specimen identifier EU-13), version 1.0, European Commission JRC, [Dataset], <https://doi.org/10.5290/180007>.
- [15] Brynk, T.; Holmström, S. (2024): Small punch tensile/fracture test data for Nimonic 75 (BCR 661) material at 21 °C and a displacement rate of .00834 mm/s (specimen identifier EU-01), version 1.0, European Commission JRC, [Dataset], <https://doi.org/10.5290/180008>.
- [16] Brynk, T.; Holmström, S. (2024): Small punch tensile/fracture test data for Nimonic 75 (BCR 661) material at 21 °C and a displacement rate of .00834 mm/s (specimen identifier EU-08), version 1.0, European Commission JRC, [Dataset], <https://doi.org/10.5290/180009>.
- [17] Brynk, T.; Holmström, S. (2024): Small punch tensile/fracture test data for Nimonic 75 (BCR 661) material at 450 °C and a displacement rate of .00834 mm/s (specimen identifier EU-03), version 1.0, European Commission JRC, [Dataset], <https://doi.org/10.5290/180010>.
- [18] Brynk, T.; Holmström, S. (2024): Small punch tensile/fracture test data for Nimonic 75 (BCR 661) material at 450 °C and a displacement rate of .00834 mm/s (specimen identifier EU-05), version 1.0, European Commission JRC, [Dataset], <https://doi.org/10.5290/180011>.
- [19] Brynk, T.; Holmström, S. (2024): Small punch tensile/fracture test data for Nimonic 75 (BCR 661) material at 450 °C and a displacement rate of .00834 mm/s (specimen identifier EU-10), version 1.0, European Commission JRC, [Dataset], <https://doi.org/10.5290/180012>.
- [20] Brynk, T.; Holmström, S. (2024): Small punch tensile/fracture test data for Nimonic 75 (BCR 661) material at 450 °C and a displacement rate of .00834 mm/s (specimen identifier EU-11), version 1.0, European Commission JRC, [Dataset], <https://doi.org/10.5290/180013>.

- [21] Brynk, T.; Holmström, S. (2024): Small punch tensile/fracture test data for Nimonic 75 (BCR 661) material at 450 °C and a displacement rate of .00834 mm/s (specimen identifier EU-14), version 1.0, European Commission JRC, [Dataset], <https://doi.org/10.5290/180014>.
- [22] Brynk, T.; Holmström, S. (2024): Small punch tensile/fracture test data for Nimonic 75 (BCR 661) material at 450 °C and a displacement rate of .00834 mm/s (specimen identifier EU-16), version 1.0, European Commission JRC, [Dataset], <https://doi.org/10.5290/180015>.
- [23] Lord J., Loveday M., Rides M., McEnteggart I., TENSTAND WP2 Final Report: Digital Tensile Software Evaluation. NPL REPORT DEPC MPE 015, <https://www.npl.co.uk/getattachment/products-services/Advanced-materials/Tensile-Testing/SW-validation-eval.pdf>.
- [24] Igor Simonovski, Stefan Holmström, Daniele Baraldi, Rémi Delville, Investigation of cracking in small punch test for semi-brittle materials, Theoretical and Applied Fracture Mechanics, Volume 108, 2020, <https://doi.org/10.1016/j.tafmec.2020.102646>.
- [25] ABAQUS 2024, Dassault Systemes, 2024.
- [26] Chakrabarty J., A theory of stretch forming over hemispherical punch heads, International Journal of Mechanical Sciences, Volume 12, Issue 4, 1970, pp. 315-325, ISSN 0020-7403, [https://doi.org/10.1016/0020-7403\(70\)90085-8](https://doi.org/10.1016/0020-7403(70)90085-8).
- [27] ASTM E3205–20, Standard Test Method for Small Punch Testing of Metallic Materials, ASTM International, West Conshohocken, PA.
- [28] Austin, T. (2024): Catalog of data from the Open Access to JRC Research Infrastructures SPT-INVEST project, version 1.0, European Commission JRC, [Catalog], <https://doi.org/10.5290/73>.
- [29] T. Melkior, D. Terentyev, C. C. Chang, A. Bakaev, S. Holmström, S. Lebediev, A. Paputsia, Mechanical properties of structural metallic alloys for nuclear applications deduced by small punch test, J. Nucl. Mater. 583 (2023), <https://doi.org/10.1016/j.jnucmat.2023.154521>.

## **Getting in touch with the EU**

### **In person**

All over the European Union there are hundreds of Europe Direct centres. You can find the address of the centre nearest you online ([european-union.europa.eu/contact-eu/meet-us\\_en](https://european-union.europa.eu/contact-eu/meet-us_en)).

### **On the phone or in writing**

Europe Direct is a service that answers your questions about the European Union. You can contact this service:

- by freephone: 00 800 6 7 8 9 10 11 (certain operators may charge for these calls),
- at the following standard number: +32 22999696,
- via the following form: [european-union.europa.eu/contact-eu/write-us\\_en](https://european-union.europa.eu/contact-eu/write-us_en).

## **Finding information about the EU**

### **Online**

Information about the European Union in all the official languages of the EU is available on the Europa website ([european-union.europa.eu](https://european-union.europa.eu)).

### **EU publications**

You can view or order EU publications at [op.europa.eu/en/publications](https://op.europa.eu/en/publications). Multiple copies of free publications can be obtained by contacting Europe Direct or your local documentation centre ([european-union.europa.eu/contact-eu/meet-us\\_en](https://european-union.europa.eu/contact-eu/meet-us_en)).

### **EU law and related documents**

For access to legal information from the EU, including all EU law since 1951 in all the official language versions, go to EUR-Lex ([eur-lex.europa.eu](https://eur-lex.europa.eu)).

### **EU open data**

The portal [data.europa.eu](https://data.europa.eu) provides access to open datasets from the EU institutions, bodies and agencies. These can be downloaded and reused for free, for both commercial and non-commercial purposes. The portal also provides access to a wealth of datasets from European countries.

# Science for policy

The Joint Research Centre (JRC) provides independent, evidence-based knowledge and science, supporting EU policies to positively impact society



**EU Science Hub**

[Joint-research-centre.ec.europa.eu](https://joint-research-centre.ec.europa.eu)



Publications Office  
of the European Union